THE JOURNAL OF BIOLOGICAL CHEMISTRY
Vol. 271, No. 40, Issue of October 4, pp. 24684–24690, 1996

Printed in U.S.A.

Spacial Compartmentalization of Ca^{2+} Signaling Complexes in Pancreatic Acini*

(Received for publication, March 8, 1996, and in revised form, May 29, 1996)

Xin Xu, Weizhong Zeng, Julie Diaz, and Shmuel Muallem‡

From the Department of Physiology, University of Texas Southwestern Medical Center, Dallas, Texas 75235

Imaging $[Ca^{2+}]_i$ at high temporal resolution and measuring the properties of Ca^{2+} signaling in streptolysin O (SLO)-permeabilized cells were used to study the spacial organization of signaling complexes. Sequential stimulation of single cells within pancreatic acini with several Ca^{2+}-mobilizing agonists revealed an agonist-specific pattern and propagation rate of Ca^{2+} waves in the same cells, with CCK8 stimulating the fastest and bombesin the slowest waves. More importantly, each agonist initiated the wave in a different region of the same cell. On the other hand, repetitive stimulation with the same agonist induced Ca^{2+} waves of the same pattern that were initiated from the same region of the cell. The agonist-specific Ca^{2+} signaling does not appear to be the result of coupling to different G proteins as infusion of an anti-Gαq antibody into the cells through a patch pipette equally inhibited Ca^{2+} signaling by all agonists. Further evidence for compartmentalization of signaling complexes was developed in permeabilized cells. The time-dependent loss of Ca^{2+} signaling due to SLO permeabilization occurred in an agonist-specific manner in the sequence cabachol > bombesin > cholecystokinin. Signaling by all agonists could be completely restored with as low as 2 μM guanosine 5′-3-*O*-(thio)triphosphate (GTPγS). At this low concentration GTPγS recoupled inositol 1,4,5-trisphosphate production and Ca^{2+} release, rather than enhancing phospholipase C activity. Priming of Ca^{2+} signaling by GTPγS was agonist-specific. Guanosine 5′-*O*-(thio)diphosphate (GDPβS) uncoupled the ability of signaling complexes to release Ca^{2+} much better than stimulating inositol 1,4,5-trisphosphate production. The uncoupling of Ca^{2+} signaling by GDPβS was also agonist-specific. The combined findings of agonist-specific initiation sites of the Ca^{2+} wave and differential access of guanine nucleotides to signaling complexes suggest spacial compartmentalization of Ca^{2+} signaling complexes. Each complex must include a receptor, G protein, and phospholipase C that are coupled to a specific portion of the Ca^{2+} pool.

Transduction of the Ca^{2+} signal can occur through G protein-coupled or G protein-independent receptor complexes (1, 2). The G protein-independent complexes are proteins containing SH2 and SH3 domains which couple plasma membrane-localized receptors to the γ isoform of phospholipase C (PLC).[1] The G protein-dependent receptor complexes use heterotrimeric G proteins from the Gq/11 family that couples plasma membrane receptors to the β isoform of PLC (1–4). Like other heterotrimeric G proteins, Gq/11 is composed of Gα and G βγ subunits (2, 4). Both subunits can activate various PLCβ isoforms (4–10) to potentially transduce different types or patterns of Ca^{2+} signaling. Additional diversity of the system is provided by the ability of a single receptor to couple to several combinations of Gα and Gβγ (11–14) to transduce different information.

A central question in recent years is how the diversity in signal transduction is manifested while maintaining specificity in cellular signaling. Many cells express a combination of signaling pathways and several receptors that activate the same signaling pathway (4). In the case of the exocrine pancreas, acinar cells respond to cholecystokinin (CCK), acetylcholine, and bombesin (BS) (15) by activation of PLC to generate IP_3 and mobilize Ca^{2+} from internal stores. How the different Ca^{2+} signaling complexes are organized and their activity coordinated is not known. Compartmentalization of signaling complexes and their communication with specific portions of the Ca^{2+} pool can be used to achieve signal specificity and control of activation. Indeed, recently we inferred such compartmentalization from the aberrant behavior of antagonists acting on streptolysin O-permeabilized pancreatic acini stimulated with GTPγS (16). To obtain further evidence for compartmentalization of signaling complexes, we measured the patterns of the $[Ca^{2+}]_i$ changes evoked by several Ca^{2+}-mobilizing agonists and their sensitivity to Gαq/11 antibodies in the same intact single cells. We also used SLO-permeable cells to determine the sensitivity of the signaling complexes to GTPγS and GDPβS. The clear differences observed with the various agonists show that agonist-specific $[Ca^{2+}]_i$ signaling can be attributed to spacial compartmentalization of signaling complexes.

MATERIALS AND METHODS

Preparation of Pancreatic Acini and Single Acinar Cells—Acini were prepared from the pancreas of 100–150-g rats by limited collagenase digestion as described previously (17). The acini were resuspended in a standard solution A containing (in mM) 140 NaCl, 5 KCl, 1 $MgCl_2$, 1 $CaCl_2$, 10 Hepes (pH 7.4 with NaOH), 10 glucose, and 0.1% bovine serum albumin, and kept on ice until use for $[Ca^{2+}]_i$ measurement in intact cells or Ca^{2+} release in permeable cells. Single acinar cells were obtained by incubation of a minced pancreas in an 0.025% trypsin, 0.02% EDTA solution for 5 min at 37 °C. After washing the tissue with solution A supplemented with 0.02% soybean trypsin inhibitor, single cells were liberated by a 7-min incubation at 37 °C in the same solution that also contained 160 units/ml pure collagenase. The cells were washed with solution A and kept on ice until use.

Measurement of $[Ca^{2+}]_i$—Acini in solution A were incubated with 5 μM Fura 2/AM for 30 min at 37 °C, washed once with solution A, and

* This work was supported by National Institutes of Health Grants DK46591 and DK38938 (to S. M.), and GM31954 (to P. Sternweis). The costs of publication of this article were defrayed in part by the payment of page charges. This article must therefore be hereby marked "*advertisement*" in accordance with 18 U.S.C. Section 1734 solely to indicate this fact.

‡ To whom correspondence should be addressed: University of Texas Southwestern Medical Center, Dept. of Physiology, 5323 Harry Hines Blvd., Dallas, TX 75235. Tel.: 214-648-2593; Fax: 214-648-8685; E-mail: smuall@mednet.swmed.edu.

[1] The abbreviations used are: PLC, phospholipase C; IP_3, inositol 1,4,5-trisphosphate; CCK, cholecystokinin; BS, bombesin; SLO, streptolysin O; GTPγS, guanosine 5′-3-*O*-(thio)triphosphate; GDPβS, guanosine 5′-*O*-(thio)diphosphate.

kept on ice until plating on glass coverslips that formed the bottom of a perfusion chamber. The plated cells were incubated for 2 min at room temperature to allow attachment to coverslips and then perfused at a rate of 10–12 ml/min for at least 10 min at 37 °C prior to the first stimulation. Acinar cell clusters consisting of three to five cells and forming a single layer in the bottom of the coverslip were selected for experimentation. Fura 2 fluorescence was measured by a PTI Int. image acquisition and analysis system as described elsewhere (18). To maximize the temporal resolution, fluorescence was measured at a single excitation wavelength of 380 nm and without image averaging. The light was directed by a dichroic mirror to an image intensifier and a video camera. The images were digitized and stored in CASH memory for further analysis. Under these conditions using a frame size of 256 × 240 pixels allowed recording the fluorescence of the entire cluster at a resolution of 2.0 Hz. A resolution of 4.7 Hz was obtained by recording the fluorescence from one cell within the cluster which could be fitted in a frame size of 128 × 120 pixels. During the perfusion with the control solution and just before the first stimulation, the image of the resting cells was acquired by averaging eight consecutive images. This was taken as the fluorescence at time 0 (F_0). All subsequent images were divided by this image, and the traces in Figs. 1–3 are the calculated F_0/F_t where F_t is the fluorescence at time t.

Measurement of Ca^{2+} Release in Permeable Cells—Agonist-mediated Ca^{2+} release from SLO-permeabilized pancreatic acini was measured exactly as described previously (16, 19). The SLO permeabilization medium was composed of Chelax-treated 145 mM KCl and 10 mM Hepes solution and supplemented with 0.02% soybean trypsin inhibitor, 3 mM ATP, 5 mM $MgCl_2$, 10 mM creatine phosphate, 5 units/ml creatine phosphokinase, 10 μM antimycin A, 10 μM oligomycin, 1 μM Fluo 3, and 3 mg/ml SLO (Difco). Fluo 3 fluorescence was recorded and calibrated as detailed previously (19).

Measurement of IP_3—IP_3 levels were measured by a radioligand assay as described elsewhere (19). Acini washed with the Chelax-treated solution and incubated in the SLO permeabilization medium with or without GDPβS, were stimulated with the indicated agonist for 20 s at 37 °C. The reactions were stopped by the transfer of 100-μl samples to 100 μl of an ice-cold 15% perchloric acid, vigorous mixing, and incubation on ice for at least 10 min to allow precipitation of proteins. The supernatants were then collected by 2-min centrifugation at 10,000 × g and transferred to clean tubes. Standards of IP_3 were prepared in permeabilization medium and processed in the same manner. The perchloric acid was removed and IP_3 extracted by the addition of 0.2 ml of Freon and 0.2 ml of tri-*n*-octylamine. After mixing and phase separation by centrifugation, between 15 and 25 μl of the upper layer were used to measure IP_3 content with microsomes prepared from bovine brain cerebella.

Whole-cell Current Recording—The tight-seal whole-cell current recording of the patch clamp technique was used (20) for measurement of Ca^{2+}-activated Cl^- current, which directly correlates with changes in $[Ca^{2+}]_i$ (21). The experiments were performed with single acinar cells perfused with solution A. The standard pipette solution contained (in mM): KCl 140, $MgCl_2$1, EGTA 0.2, Na_2 ATP 5, and Hepes 10 (pH 7.3 with KOH) as described in previous studies (21). In some experiments this solution also contained either 80 μg/ml preimmune serum or IgG anti-Gαq/11 antibodies, both of which were a generous gift from Dr. Paul Sternweis, University of Texas Southwestern Medical Center, Dallas (22). Seals of 6–10 gigohms were produced on the cell membrane, and the whole cell configuration was obtained by gentle suction or voltage pulses of 0.5 V for 0.3–1 ms. The patch clamp output (Axopatch-1B, Axon Instruments) was filtered at 20 Hz. Recording was performed with patch clamp 6 and a Digi-Data 1200 interface (Axon Instruments). The cells were voltage clamped at −30 mV, and depolarizing voltage jumps of 100-ms duration at a frequency of 1 Hz to a membrane potential of +10 mV were applied throughout the experiments to measure the leak current. In all experiments the Cl^- and cation equilibrium potentials were about 0 mV. All the traces shown were at a holding potential of −30 mV and were corrected for leak currents.

RESULTS

Agonist Specific Initiation Sites of Ca^{2+} Release—Pancreatic acini express several distinct receptors for Ca^{2+} mobilizing agonists in the basolateral membrane, which stimulate the exocytotic secretion of digestive enzymes through the apical membrane (15). The most potent Ca^{2+}-mobilizing agonists are acetylcholine, bombesin, and CCK, all of which cause a large increase in IP_3 to mobilize all the agonist-sensitive intracellular Ca^{2+} pool (15, 23–26). Mobilization of Ca^{2+} from internal stores by one of these agonists, acetylcholine, was shown to be initiated in the apical and spread to the basolateral pole of the cell (27–29). To determine whether all agonists acting on acinar cells initiate the Ca^{2+} signal at the same site, we compared the effects of the three agonists on $[Ca^{2+}]_i$ of the same cells. All the experiments were performed on clusters of three to five cells to ensure the maintenance of intact tight junctions and cellular polarity, and then $[Ca^{2+}]_i$ was analyzed in single cells within the cluster. Fig. 1 shows the experimental protocol used. The cells were stimulated with supermaximal concentration of agonists to mobilize all the Ca^{2+} in the intracellular stores. Shortly after stimulation, the cells were inhibited with the relevant antagonist to force Ca^{2+} back into the intracellular stores and cause rapid and maximal reloading (25, 30, 31). In the first set of experiments images were collected from the entire acinus at a resolution of 2.0 Hz, which was sufficient to determine the rate of the Ca^{2+} wave. The *upper panel* of Fig. 1 shows the averaged $[Ca^{2+}]_i$ changes in the entire cell. The *bottom panels* show the rising phase of $[Ca^{2+}]_i$ for each agonist in an expanded time scale. In each case the *solid line* depicts the $[Ca^{2+}]_i$ in the initiation region and the *dashed line* in the region in which $[Ca^{2+}]_i$ increased last. In all experiments CCK8 caused the fastest and bombesin the slowest $[Ca^{2+}]_i$ waves. In 34 cells from nine experiments the waves initiated by CCK8, carbachol, and bombesin propagated within 0.47 ± 0.06, 0.92 ± 0.13, and 2.3 ± 0.15 s, respectively.

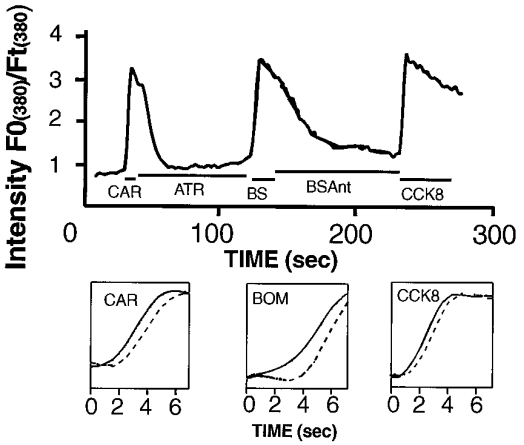

FIG. 1. **Agonist-specific propagation rate of Ca^{2+} waves in single pancreatic acinar cells.** A Fura 2 loaded cluster of four acinar cells was stimulated with 100 μM carbachol (*CAR*). When $[Ca^{2+}]_i$ was maximal, the cells were inhibited with 10 μM atropine (*ATR*). Where indicated, the cells were then stimulated with 25 nM BS and at peak $[Ca^{2+}]_i$ inhibited with 100 nM of the bombesin antagonist [D-Phe^6,Des-Met^{14}]-BS (6–14), ethyl amide (Bachem California, Torrance, CA) (*BSAnt*). Finally the cells were stimulated with 10 nM CCK8. The changes in $[Ca^{2+}]$ were analyzed in multiple areas of each cell to determine the first and last regions of $[Ca^{2+}]_i$ increase and the time required for the wave to propagate between these regions. The *bottom panels* show the rising phase of $[Ca^{2+}]_i$ for each agonist in one of the four cells. In each case the *solid line* depicts the first region and the *dashed line* the last region of $[Ca^{2+}]_i$ increase. In the experiment shown, the first $[Ca^{2+}]_i$ increase for all agonists was in the luminal and the last increase in the basal region of the cell.

To further analyze the differences between the agonists, the same protocol was used but now $[Ca^{2+}]_i$ was imaged in one cell and only during the rising phase at a resolution of 4.7 Hz (maximal possible with our recording system). Fig. 2 shows the results of such an experiment. The *upper bright-field image* is a 600 × magnification of the three-cell cluster used for the experiment. The *bottom left panel* shows a 1000 × magnification of the cell enclosed by the *broken line* in the 600 × image. The remaining images are the Fura 2 fluorescence ratios re-

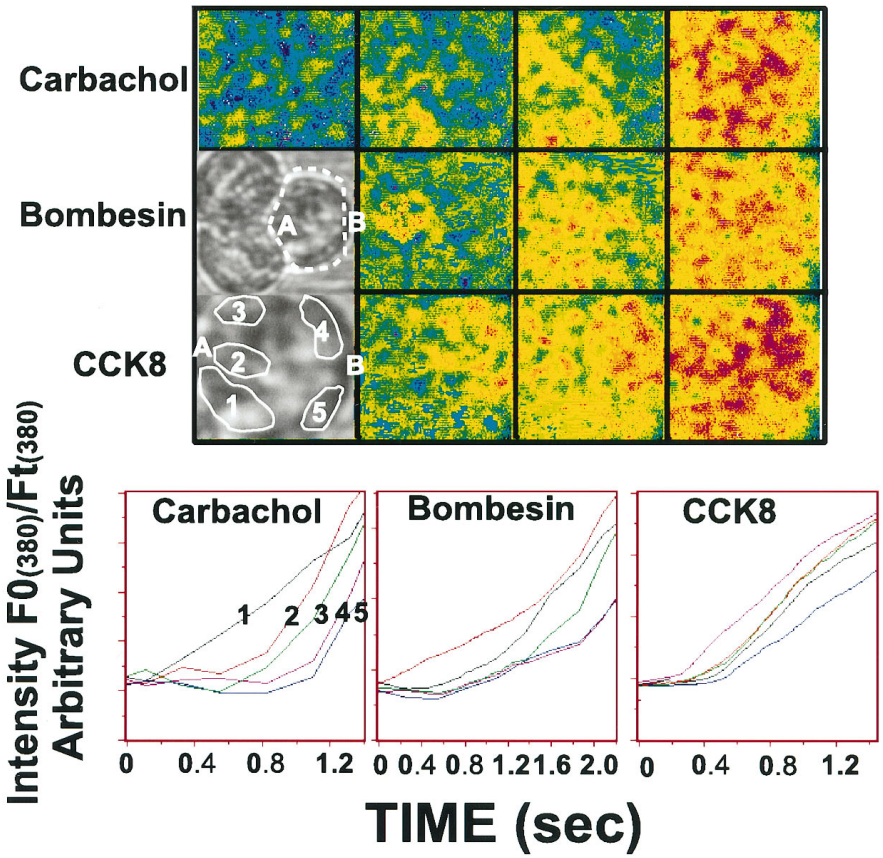

FIG. 2. **Agonist-specific initiation and patterns of $[Ca^{2+}]_i$ waves in single pancreatic acinar cells.** The experimental protocol was similar to that in Fig. 1 except that a three-cell cluster (*middle left*, magnification, × 600) was used and Fura 2 fluorescence was recorded only during the rising phase of $[Ca^{2+}]_i$ from one of these cells, as marked by the *dashed line* in the *middle left panel* and shown in × 1000 magnification in the *bottom left panel*. Fluorescence imaging was performed at the × 1000 magnification used to record the bright-field image in the *bottom left*. Fluorescence image ratios are displayed in pseudocolor. The *top left panel* shows the $[Ca^{2+}]_i$ of the cell under resting conditions. The remaining images in the *upper row* show three images recorded during stimulation of the cell with 100 μM carbachol. The fluorescence images in the *middle row* are from the period of stimulation with 25 nM bombesin and the fluorescence images in the *bottom row* are from the period of stimulation with 10 nM CCK8. The *bottom panels* show the change in F_0/F_t fluorescence ratios during the first 1.4 or 2.2 s of the $[Ca^{2+}]_i$ rise phase for each agonist. *Traces 1–5* show the $[Ca^{2+}]_i$ changes in the areas marked *1–5* in the *bottom left*, bright-field image. The apical (*A*) and basal (*B*) poles of the cells are also marked.

corded at a magnification of 1000 × and at an excitation wavelength of 380 nm. The *top left image* was recorded under resting conditions. The second row of images shows the first detected $[Ca^{2+}]_i$ increase when the same cell was stimulated with carbachol (*top*), bombesin (*middle*), or CCK8 (*bottom*). The next row shows images for each agonist when the $[Ca^{2+}]_i$ spread through about one-half of the cell. The row on the right shows the first images when maximal Ca^{2+} increase was achieved for each agonist, which demonstrates that each agonist was able to access the entire cellular Ca^{2+} pool. It is clear that in the experiment shown each agonist initiated the $[Ca^{2+}]_i$ increase in different areas of the cell. In five of seven similar experiments, all three, and in two of seven experiments, two of the three, agonists initiated the $[Ca^{2+}]_i$ increase in different areas of the same cell. Since the spread of the Ca^{2+} wave (see above) is significantly slower than the recording resolution, it is unlikely that the agonist-specific initiation sites were due to inadequate spacial resolution. Agonist-specific initiation sites were frequently observed when the recording resolution was under the condition of Fig. 1. Under this condition the fluorescence of the entire cell cluster could be recorded and again in 34 cells from nine clusters at least two of the three agonists initiated the $[Ca^{2+}]_i$ increase in different areas of the same cell.

Another difference between the agonists is the pattern of the Ca^{2+} wave as illustrated in the traces in the *bottom panels* of Fig. 2. The traces show the pattern of $[Ca^{2+}]_i$ changes during the first 1–2 s of cell stimulation for each agonist. The carbachol-induced $[Ca^{2+}]_i$ wave propagated from *areas 1* to *2*, *3*, *4*, and *5*. The bombesin-induced wave appears to progress simultaneously in two directions increasing first at area 2 and then at areas 1 and 3 at about the same time and then at areas 4 and 5. The CCK8-induced wave was almost in the opposite direction from that of carbachol, starting at area 4 and rapidly progressing through areas 3, 2, 1, and then 5. Similar agonist-specific patterns were recorded in the experiments mentioned above that were designed to identify the initial site of $[Ca^{2+}]_i$ increase for each agonist. As reported before for acetylcholine (27–29), carbachol and bombesin always initiated the $[Ca^{2+}]_i$ increase in the apical region (marked with *A* in bright-field images) and the wave tended to spread through the cell periphery to the basal region (marked with *B*). In the case of CCK8 the $[Ca^{2+}]_i$ increase was initiated either in the apical (Fig. 1) or basolateral (Fig. 2) regions, although in most experiments (~76%) it started in the apical region of the cell.

An important control experiment in assigning a specific portion of the pool to a Ca^{2+}-mobilizing agonist is to demonstrate that repetitive stimulation with the same agonist initiates Ca^{2+} waves of the same pattern and from the same region of the cytoplasm. To demonstrate this behavior, we selected carbachol, since stimulation by this agonist can be readily reversed with a very low concentration of atropine, and atropine can then be easily washed to allow repetitive stimulations. Fig.

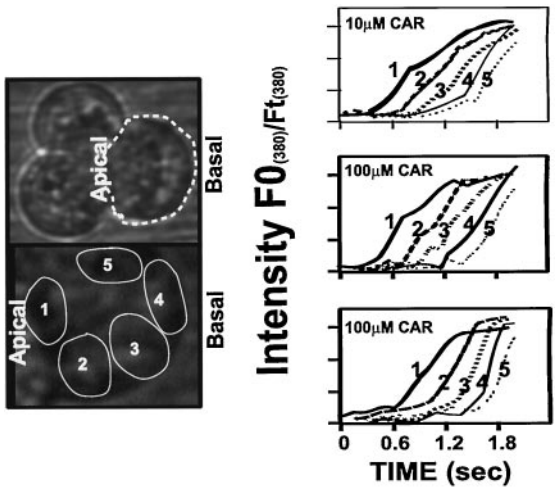

FIG. 3. **Constant initiation site and pattern of $[Ca^{2+}]_i$ waves induced by repetitive stimulation with the same agonist.** The *upper* and *lower* bright-field images are the × 600 and × 1000 magnification of the cluster and the cell from which fluorescence was recorded, respectively. The *dotted line* in the upper image marks the cell shown in the lower image. The apical and basal pole of the cluster and the cells are indicated. *Regions 1–5* in the lower image indicate the areas analyzed. The corresponding traces are shown in the *right panel*. For this experiment the cell was stimulated first with 10 μM carbachol (*CAR*), and at peak $[Ca^{2+}]_i$ it was inhibited with 2 nM atropine. After an additional 5.5 min of continuous perfusion at 37 °C with solution A, the cell was stimulated with 100 μM carbachol and at peak $[Ca^{2+}]_i$ inhibited with 2 nM atropine. Finally, after an additional 5.5-min perfusion with solution A, the cell was restimulated with 100 μM carbachol. The traces show the changes in $[Ca^{2+}]_i$ during 1.8 s of the $[Ca^{2+}]_i$ rising phase in regions 1–5.

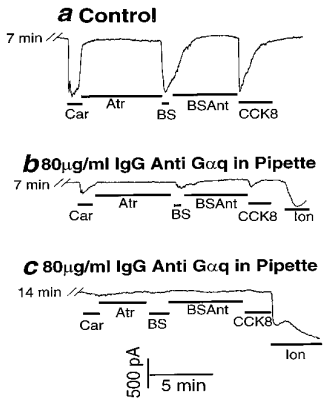

FIG. 4. **Effect of anti-Gαq antibody on Ca^{2+} signaling by all agonists.** The Ca^{2+} activated Cl^- current was recorded as described under "Materials and Methods." In experiment *a*, the pipette solution contained 80 μg/ml preimmune serum, whereas in experiments *b* and *c* the pipette solution contained 80 μg/ml IgG anti-Gαq/11 antibody. After either 7 (*a* and *b*) or 14 (*c*) min of cytosolic perfusion with the pipette solutions, the cells were sequentially exposed to 100 μM carbachol (*Car*), 10 μM atropine (*Atr*), 25 nM BS, 100 nM bombesin antagonist (*BSAnt*), and 10 nM CCK8. To show that the antibody had no effect on the channel itself, the cells were exposed to 2 μM ionomycin (*Ion*) (*b* and *c*) to elevate $[Ca^{2+}]_i$ and activate the current. The number of experiments and controls performed are listed in the text.

3 shows the results of such an experiment. The acinus (*top image*) was stimulated once with maximal and twice with supermaximal concentrations of carbachol. At the $[Ca^{2+}]_i$ peak, stimulation was terminated with 2 nM atropine, and then atropine was washed for at least 5 min before a second stimulation was attempted. Recording and analysis of $[Ca^{2+}]_i$ changes in different regions of one of the cells (*bottom image*) clearly showed that, on repetitive stimulation, carbachol always increased $[Ca^{2+}]_i$ first at region 1 of the apical pole and then the wave propagated in the direction 1, 2, 3, 4, and 5. In addition, the rate of wave propagation was very similar at each stimulation. Identical results in terms of the initiation site and wave pattern were obtained in four additional experiments. At submaximal agonist concentrations that still accessed the entire Ca^{2+} pool, the rate of wave propagation was slower than at maximal agonist concentration, but the initiation site and wave pattern were identical at all agonist concentrations (not shown, $n = 4$). Hence, in all experiments performed with no exception, repetitive stimulation with the same agonist resulted in wave initiation from the same site.

Coupling to Gαq—The agonist-specific initiation, pattern, and speed of the $[Ca^{2+}]_i$ wave can be due to spacial compartmentalization of signaling complexes and/or coupling to different α subunits of the heterotrimeric G proteins. We examined to some extent the role of Gα subunits in conferring specificity by determining the sensitivity of Ca^{2+} signaling by the various agonists to inhibition of the action of Gαq/11. Fig. 4 shows the results of such experiments. An IgG anti-Gαq/11 was infused into the cell through a patch pipette, and $[Ca^{2+}]_i$ was followed by measuring the activity of the Ca^{2+}-activated Cl^- channel. This technique was extensively used to follow $[Ca^{2+}]_i$ changes next to the plasma membrane of various secretory cells (21). Preliminary experiments showed that when the pipette solution contained between 80–240 μg/ml IgG anti-Gαq/11 (the highest concentration tested) maximal inhibition of Ca^{2+} signaling could be achieved. Concentrations of the antibody between 80 and 240 μg/ml affected only the time of dialysis required to achieve maximal inhibition. In Fig. 3, 80 μg/ml IgG was used. *Trace b* shows an experiment in which less than maximal inhibition was achieved. The trace is shown to demonstrate that the Gαq/11 antibody inhibited the signal induced by the three agonists to a similar extent. The effect of carbachol was inhibited by 82%, that of bombesin by 86%, and that of CCK8 by 87%. In *trace c* the anti-Gαq/11 antibody inhibited the effect of all the agonists by more than 95%. The antibody inhibited Ca^{2+} signaling by all agonists and to a similar extent in all 17 experiments tested. Thus, it appears that all three receptors are coupled to Gαq.

Compartmentalized Signaling Complexes in Permeable Cells—Spacial compartmentalization of signaling complexes was supported by testing the time-dependent effect of cell permeabilization with SLO toxin on Ca^{2+} signaling by the three agonists. As we reported before (16, 19), after permeabilization with SLO, pancreatic acinar cells retain intact signaling systems, including the stimulated generation of IP_3 and Ca^{2+} release from intracellular stores. However, continuous exposure to SLO resulted in a time-dependent loss of signaling, which was agonist-specific. Fig. 5 shows individual experiments with carbachol and CCK8, whereas Fig. 6 (*closed symbols*) summarizes the results of three to six experiments with all agonists. The ability of carbachol to signal Ca^{2+} release was lost within 10 min of exposure to SLO. The lose of signaling by bombesin was slower with 60% inhibition after 10-min incubation with SLO, while CCK8 signaling was quite resistant to permeabilization by SLO with only about a 20% loss of signaling after 10 min of permeabilization.

The loss of Ca^{2+} signaling could be completely restored by the addition of very low concentration of GTPγS. Fig. 7 shows individual experiments in which the cells were stimulated with carbachol or CCK8 and 2 μM GTPγS after 2 or 10 min of permeabilization with SLO. Fig. 6 (*open symbols*) summarizes the results obtained with all agonists after 10 min permeabilization. It is clear that the low concentration of GTPγS was able to restore maximal signaling by all agonists. G proteins can affect Ca^{2+} signaling either by regulating PLC and IP_3 production (4), or by directly regulating the IP_3-activated Ca^{2+} chan-

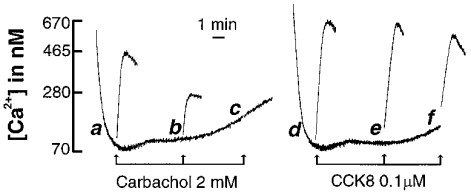

FIG. 5. **Effect of permeabilization with SLO on carbachol or CCK8-induced Ca^{2+} signaling.** Acini were incubated in SLO permeabilization medium for about 1.5 (*a* and *b*), 5 (*b* and *e*), or 10 min (*c* and *f*) at 37 °C prior to stimulation with either 2 mM carbachol (*a–c*) or 0.1 μM CCK8 (*d–f*). The continuous traces are from experiments *c* and *f* and show the [Ca^{2+}] of the incubation medium during the 10-min incubation at 37 °C. All the experiments performed are summarized in Fig. 6.

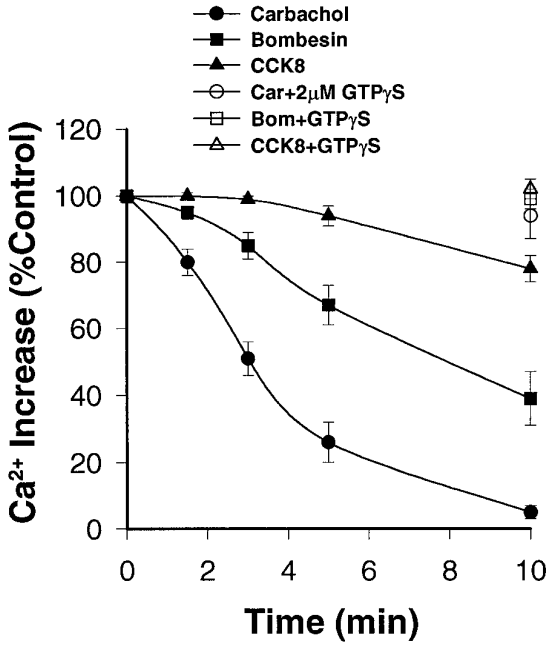

FIG. 6. **Time course of agonist-dependent Ca^{2+} signaling loss by SLO permeabilization.** Protocols similar to those in Figs. 5 and 7 were used to evaluate the loss of Ca^{2+} signaling by each agonist. After the indicated permeabilization periods, the cells were stimulated with 2 mM carbachol (●), 2 mM carbachol and 2 μM GTPγS (○), 0.1 μM bombesin (■), 0.1 μM bombesin and 2 μM GTPγS ([□]), 0.1 μM CCK8 (▲), or 0.1 μM CCK8 and 2 μM GTPγS (△). The figure shows the mean ± S.E. of three to six experiments.

nel (32). To distinguish between the two possibilities we measured the effect of SLO permeabilization on IP_3 production. Table I shows that after 2-min permeabilization with SLO all agonists increase IP_3 levels to the same extent and 2 μM GTPγS had no effect on IP_3 production. A more significant finding is that after 10-min permeabilization IP_3 production by all agonist was equally reduced by about 25–30% and GTPγS did not restore IP_3 production to control levels. Thus, the loss or uncoupling of a GTP-dependent mechanism downstream from PLC stimulation was specific for the signaling complex of each agonist.

The effects of GTPγS described above prompted us to test the sensitivity of signaling by the three agonists to GDPβS. Individual experiments with carbachol and bombesin are shown in Fig. 8, while Fig. 9*A* summarizes the results of four experiments. In all experiments the sensitivity to GDPβS was tested after 2 min of permeabilization, and GDPβS was included in the permeabilization medium to ensure uniformity of conditions. The differences between the agonists are quite clear. GDPβS inhibited carbachol-induced Ca^{2+} release with an IC_{50} of about 0.042 mM, bombesin-induced Ca^{2+} release with an IC_{50} of about 0.53 mM, and CCK8-induced Ca^{2+} with an IC_{50} of about 1.48 mM. Hence, GDPβS has different access to the Ca^{2+} signaling complexes coupled to the carbachol, bombesin, and CCK receptors.

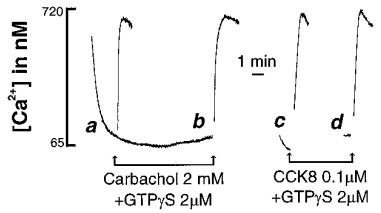

FIG. 7. **Restoration of agonist-mediated Ca^{2+} signaling by GTPγS.** Acini were incubated in SLO permeabilization medium for about 2 (*a* and *c*) or 10 min (*b* and *d*) at 37 °C before stimulation with either 2 mM carbachol and 2 μM GTPγS (*a* and *b*) or 0.1 μM CCK8 and 2 μM GTPγS (*c* and *d*). The changes in medium [Ca^{2+}] during the 10-min incubation at 37 °C is shown only for *trace b*. All the experiments performed are summarized in Figure 6.

TABLE I

Effect of incubation time in SLO on agonist-stimulated IP_3 production

Acini incubated in the SLO-permeabilization medium for either 2 or 10 min at 37 °C were stimulated with the indicated agonist and with or without 2 μM GTPγS for 20 s.

Conditions	Incubation Time (min)	
	2	10
	IP_3 in pmol/mg protein	
Control	4.3 ± 0.2[a]	4.7 ± 0.4
2 μM GTPγS	4.7 ± 0.3	4.7 ± 0.2
Carbachol 2 mM	64 ± 6	45 ± 3
+ GTPγS 2 μM	69 ± 8	52 ± 2
Bombesin 0.1 μM	62 ± 4	43 ± 2
+ GTPγS 2 μM	65 ± 5	48 ± 3
CCK 8 0.1 μM	71 ± 3	51 ± 4
+ GTPγS 2 μM	72 ± 2	54 ± 2

[a] Values are the mean ± standard error of the mean of triplicate determinations. Similar results were obtained in three additional experiments.

To determine if the inhibition of Ca^{2+} signaling by GDPβS was due to inhibition of PLC we measured the effect of GDPβS on IP_3 production. Fig. 9*B* shows that inhibition by GDPβS was agonist-specific. However, much higher GDPβS concentrations were needed to inhibit IP_3 production (Fig. 9*B*) than Ca^{2+} release (Fig. 9*A*). Even at 2.5 mM, GDPβS had no effect on IP_3 production stimulated by CCK8. GDPβS only partially inhibited the effect of bombesin with about 32% inhibition at 2.5 mM. In the case of carbachol, GDPβS inhibited IP_3 production by approximately 65% with an IC_{50} of 0.53 mM, which is about 13-fold higher than that required for 100% inhibition of Ca^{2+} release (Fig. 9*A*).

DISCUSSION

Multiple receptor types that use the same transduction system and second messengers are present in virtually every cell type (1, 2, 4). Cross-talk between the same and different signaling pathways has been known for many years (1, 4). Most recently such cross-talk was demonstrated between heterotrimeric G proteins and tyrosine kinase-dependent pathways (33, 34). The extensive and coupled network of signaling pathways requires mechanisms to achieve specificity and precision in signal transduction. Compartmentalization of signaling by localization of several (or all) components of signaling complexes is emerging as a control mechanism in achieving signaling specificity. For example, many components of the mitogen-activated protein kinase and other signaling pathways are clustered in caveolae (35, 36). In the case of Ca^{2+} signaling, differential localization of protein kinase C isoforms is used to regulate different cellular activities (37). Clustering of specific Ca^{2+} channels by binding to components of the exocytotic path-

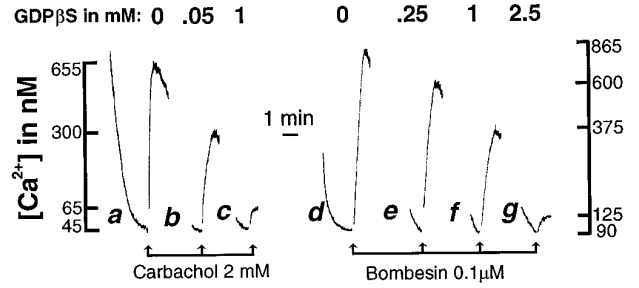

FIG. 8. **Effect of GDPβS on Ca^{2+} signaling in SLO permeabilized cells.** Acini were incubated in SLO permeabilization medium containing 0 (*a* and *d*) 0.05 (*b*), 0.25 (*e*), 1 (*c* and *f*), or 2.5 mM GDPβS (*g*) for about 2 min at 37 °C. Where indicated, the cells were then stimulated with 2 mM carbachol (*a–c*) or 0.1 μM bombesin (*d–g*). All the experiments performed are summarized in Fig. 9.

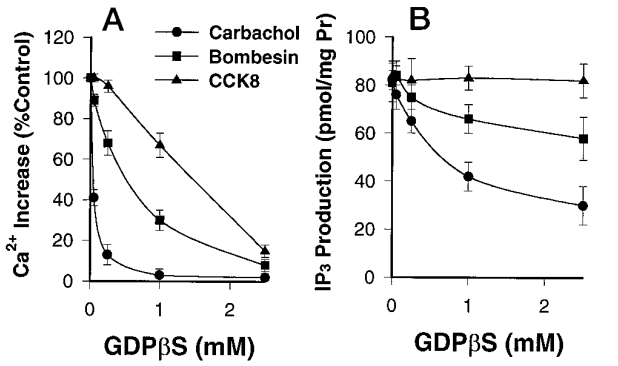

FIG. 9. **Effect of GDPβS on agonist stimulated Ca^{2+} signaling and IP_3 production.** *Panel A*, the protocols of Fig. 8 were used to determine the effect of GDPβS on Ca^{2+} release by 2 mM carbachol (●), 0.1 μM bombesin (■), or 0.1 μM CCK8 (▲). The figure shows the mean ± S.E. of four separate experiments. *Panel B*, acini were incubated in the SLO permeabilization medium containing between 0 and 2.5 mM GDPβS for 2 min at 37 °C before a 20-s stimulation with 2 mM carbachol (●), 0.1 μM bombesin (■), or 0.1 μM CCK8 (▲). The reactions were stopped by transferring cells to a solution containing perchloric acid to analyze the levels of IP_3 by radioimmunoassay as described under "Materials and Methods." The figure shows the mean ± S.E. of three experiments performed in duplicate determinations.

way is believed to control the site of neurotransmitter release (38, 39).

The problem of Ca^{2+} signaling specificity is somewhat more acute in polarized secretory cells such as pancreatic and other acinar cells. For the most part receptors in the basolateral membrane transduce their signal to the apical membrane, where exocytosis of digestive enzymes and fluid secretion occurs (15). A partial solution to signaling specificity appears to be compartmentalization of the Ca^{2+} pool which results in quantal behavior of Ca^{2+} release (40) and localized changes in $[Ca^{2+}]_i$ next to the apical membrane (27, 28). In the present studies we extended the previous findings (27–29) to show that all major Ca^{2+}-mobilizing agonists release Ca^{2+} first in the apical region which then propagates to the basolateral region. A difference between our studies and those reported before (27, 28) is that we used clusters of three to five cells to ensure intact tight junctions and the maintenance of cell polarity, whereas previous studies (27, 28) used single isolated cells. The use of cell clusters showed that the initial increase in Ca^{2+} tended to occur in the boundary between the basolateral and the apical membrane. In addition we find that, at least in the case of CCK receptors, the $[Ca^{2+}]_i$ wave can start in several regions of the cell, such as the apical, apical-lateral or lateral-basal regions (Fig. 2). These features suggest that the receptors for all agonists can be clustered in regions of the basal or lateral membranes from which they initiate localized Ca^{2+} signal close to the apical membrane. Thus, the Ca^{2+} liberating messenger IP_3 does not need to diffuse across the cell to initiate the Ca^{2+} signal in the apical region. Rather, it can act at the site of its production by the clustered receptors. Clustering of the receptors can be viewed as the first order of signal compartmentalization.

Another aspect of signal specificity was revealed when the initiation, pattern and propagation of the Ca^{2+} signal evoked by each agonist was studied in the same cell. Previous studies have already shown that carbachol and CCK can initiate different patterns of Ca^{2+} spiking in acinar cells (41). At low agonist concentration this Ca^{2+} spiking can be confined to one pole of the cells (27, 28). Here we used supermaximal concentrations of agonists to access all the Ca^{2+} pool by each agonist to determine whether a) agonist specificity is maintained when IP_3 production is not limited and b) to be able to follow the initiation and propagation of the wave in the entire cell. The protocol of Fig. 1 revealed that each agonist initiates the Ca^{2+} signal in different region of the cell, even when high agonist concentrations are used. In addition, the pattern and propagation rate for each Ca^{2+} wave differs among the agonists used. The simplest interpretation of these findings is compartmentalization of the Ca^{2+} pool and coupling of individual compartments to specific signaling complexes. This coupling must be very tight as repetitive stimulation of the same cell with maximal or different concentrations of the same agonist always initiated the $[Ca^{2+}]_i$ wave at the same cellular site. In previous studies we provided evidence for such an arrangement in SLO-permeabilized cells (16, 19). Compartmentalized pools with variable affinities for IP_3 could be accessed by all antagonists in permeabilized but not intact cells (16). Furthermore, in salivary gland ducts isoprenaline, carbachol and ATP access non overlapping and limited portions of the internal Ca^{2+} pool, whereas isoproterenol and forskolin access the same overlapping portion of the pool (42). Compartmentalization of the pool and its coupling to specific signaling complexes can be viewed as the second order of signal compartmentalization.

A more direct evidence for spacial compartmentalization of signaling was obtained by studying the properties of Ca^{2+} signaling in permeable cells. Cell permeabilization with SLO caused time-dependent lose of Ca^{2+} signaling with the sequence (first to last) carbachol, bombesin, CCK. Signaling by all agonists could be completely restored at any time after permeabilization with low concentration of GTPγS. GTP was much less efficient than GTPγS in restoring signaling (not shown) despite the presence of an ATP/GTP regeneration system in the reaction medium. A tentative interpretation of these experiments is that the signaling complexes lose GTP needed for activation of G proteins at different rates. This is, however, not likely since ATP and IP_3 have complete access to the Ca^{2+} pump and the Ca^{2+} channel, respectively, a short time after cell permeabilization (16, 19). Heparin with a molecular mass of 6 kDa completely inhibits Ca^{2+} release induced by IP_3 and all agonists (ref 16 for carbachol and CCK8 and not shown for bombesin). The 5-kDa β thymosins and a 15-kDa S1 fragment of gelsolin can access the actin in the basal and luminal membranes (43). In addition, it is difficult to comprehend how GDPβS can access the signaling complexes (albeit at high concentrations) while GTP, which is likely to be in the μM range, will be retained by the CCK signaling complex. Indeed, the loss of Ca^{2+} signaling by carbachol and bombesin was not accompanied by a loss in the ability to activate a Gαq-coupled PLC and generate IP_3, nor the ability of GTPγS to restore signaling was reflected in an increased agonist stimulated IP_3 production (Table I).

A more likely explanation for the loss of signaling and its

restoration by GTPγS may lie in our recent findings, showing a dual role for G proteins in Ca^{2+} signaling; activation of PLC and regulation of the coupling between IP_3 production and Ca^{2+} release (32). Thus, it is possible that incubation in SLO leads to a time-dependent uncoupling between agonist-stimulated IP_3 production and Ca^{2+} release, which can be restored by low [GTPγS] and inhibited by GDPβS. The rate of uncoupling in SLO is different for the various agonists. The agonist-specific uncoupling points to strict spacial compartmentalization of signaling complexes which must include, for each agonist, a receptor, a G protein, an effector (PLC), IP_3, and its access to specific portion of the internal pool.

In summary, we used the measurement of $[Ca^{2+}]_i$ at relatively high time resolution in the same single cells stimulated with several Ca^{2+} mobilizing agonists and characterized several properties of Ca^{2+} signaling by the various agonists in SLO-permeabilized cells to conclude the spacial compartmentalization of Ca^{2+} signaling complexes. Such compartmentalization is likely to be important in determining signaling specificity. Thus, the site of action of second messengers can be determined by compartmentalization so that the same second messenger can modulate different cellular activities or the same activities at different sites. We also provide evidence for multiple roles for G proteins in Ca^{2+} signaling, which regulate IP_3 production and the ability of IP_3 to release Ca^{2+} from internal stores.

Acknowledgments—We thank Dr. Paul Sternweis for generously providing the anti-Gαq/11 antibodies and control serum. We thank Mary Vaughn for expert administrative support.

REFERENCES

1. Berridge, M. J. (1993) *Nature* **361,** 315–325
2. Hepler J. R., and Gilman G. (1992) *Trends Biochem. Sci.* **17,** 383–387
3. Clapham, D. E., and Neer, E. J. (1993) *Nature* **365,** 403–406
4. Neer, E. J. (1995) *Cell* **80,** 249–257
5. Berstein, G., Blank, J. L., Smrcka, A. V., Higashijima, T., Sternweis, P. C., Exton, J. H., and Ross, E. M. (1992) *J. Biol. Chem.* **267,** 8081–8088
6. Loessberg, P. A., Zhao, H., and Muallem, S. (1991) *J. Biol. Chem.* **266,** 1363–1366
7. Taylor, S. J., Chae, H. Z., Rhee, S. G., and Exton, J. H. (1991) *Nature* **350,** 516–518
8. Harden, K. T. (1992) *Adv. Second Messenger Phosphoprotein Res.* **26,** 11–34
9. Camps, M., Carozzi, A., Schnable, P., Scheer, A., Parker, P. J., and Gierschik, P. (1992) *Nature* **360,** 684–686
10. Smrcka, A. V., and Sternweis, P. C. (1993) *J. Biol. Chem.* **268,** 9667–9674
11. Abou-Samra, A.-B., Juppner, H., Force, T., Freeman, M. W., Kong, X.-F., Schipani, E., Urena, P., Richards, J., Bonventre, J. V., Potts, J. T., Jr., Kronenberg, H. M., and Segre G. V. (1992) *Proc. Natl. Acad. Sci. U. S. A.* **89,** 2732–2736
12. Kleuss, C., Hescheler, J., Ewel, C., Rosenthal, W., Schultz, G., and Wittig, B. (1991) *Nature* **353,** 43–48
13. Kluess, C., Scherubl, H., Hescheler, J., Schultz, G., and Wittig, B. (1992) *Nature* **358,** 424–426
14. Kleuss, C., Scherubl, H., Hescheler, J., Schultz, G., and Wittig, B. (1993) *Science* **259,** 832–834
15. Williams, J. A., and Yule, D. I. (1993) in *The Pancreas, Biology, Pathobiology and Disease* (Go, V. L., ed) pp. 167–189, Raven Press, New York
16. Tortorici, G., Zhang, B.-X., Xu, X., and Muallem, S. (1994) *J. Biol. Chem.* **269,** 29621–29628
17. Xu, X., Star, R. A. Tortorici, G., and Muallem, S. (1994) *J. Biol. Chem.* **269,** 12645–12653
18. Stauffer, P. L., Zhao, H., Luby-Phelps, K., Moss, R. L., Star, R. A., and Muallem, S (1993) *J. Biol. Chem.* **268,** 19769–19775
19. Zhang, B.-X., Tortorici, J., Xu, X., and Muallem, S. (1994) *J. Biol. Chem.* **269,** 17132–17135
20. Hamill, O. P., Marty, A., Neher, E., Sakmann, B., and Sigworth, F. J. (1981) *Pflugers Arch.* **391,** 85–100
21. Petersen, O. H. (1992) *J. Physiol.* **448,** 1–51
22. Gutowski, S., Smrcka, A., Nowak, L., Wu, D., Simon, M., and Sternweis, P. C. (1991) *J. Biol. Chem.* **266,** 20519–20524
23. Muallem, S. (1992) *Adv. Second Messenger Phosphoprotein Res.* **26,** 351–368
24. Muallem, S., Schoeffield, M., Fimmel, C. J., and Pandol, S. (1988) *Am. J. Physiol.* **255,** G229–G235
25. Pandol, S. Schoeffield, M. S., Fimmel, C. J., and Muallem, S. (1987) *J. Biol. Chem.* **262,** 16963–16968
26. Pandol, S. J., Schoeffield M. S., Sachs, G., and Muallem, S. (1985) *J. Biol. Chem.* **260,** 10081–10086
27. Thorn, P., Lawrie, A. M., Smith, P. M., Gallacher, D. V., and Petersen, O. H. (1993) *Cell* **74,** 661–668
28. Kasai, H., Li, Y. X., and Miyashita, Y. (1993) *Cell* **74,** 669–677
29. Nathanson, M. H., Padfield, P. J., O'Sullivan, A. J., Burgstahler, A. D., and Jamieson, J. D. (1992) *J. Biol. Chem.* **267,** 18118–18121
30. Muallem, S., Pandol, S., and Beeker, T. G. (1988) *Biochem. J.* **255,** 301–307
31. Muallem, S., Kahdemazad, M., and Sachs, G. (1990) *J. Biol. Chem.* **265,** 2011–2016
32. Xu, X., Zeng, W.-Z., Muallem, S. (1996) *J. Biol. Chem.* **271,** 18520–18526
33. Lev, S., Moreno, H., Martinez, R., Canoll, P., Peles, E., Musacchio, J. M., Plowman, G. D., Rudy, B., and Schlessinger, J. (1995) *Nature* **376,** 737–745
34. Van Blesen, T., Hawes, B. E., Luttrell, D. K., Krueger, K. M., Kazushige, T., Porfirl, Sakaue, M., Luttrell, L. M., and Lefkowitz (1995) *Nature* **376,** 781–784
35. Anderson, R. G. (1993) *Curr. Opin. Cell Biol.* **5,** 647–652
36. Anderson, R. G. (1993) *Proc. Natl. Acad. Sci. U. S. A.* **90,** 10909–10913
37. Mochly-Rosen, D. (1995) *Science* **268,** 247–251
38. Sheng, Z.-H., Rettig, J., Cook, T., and Catterall, W. A. (1996) *Nature* **379,** 451–454
39. Sudhof, T. C. (1995) *Nature* **375,** 645–653
40. Muallem, S., Pandol, S. J., and Beeker, T. G. (1989) *J. Biol. Chem.* **264,** 205–212
41. Yule, D. I., Lawrie, A. M., and Gallacher, D. V. (1991) *Cell Calcium* **12,** 145–151
42. Xu, X., Diaz, J., Zhao, H., and Muallem, S. (1996) *J. Physiol.* **491,** 647–662
43. Muallem, S., Kwiatkowska, K., Xu, X., and Yin, H. L. (1995) *J. Cell Biol.* **128,** 589–598

Cell Biology and Metabolism:

Spacial Compartmentalization of Ca^{2+} Signaling Complexes in Pancreatic Acini

Xin Xu, Weizhong Zeng, Julie Diaz and Shmuel Muallem

J. Biol. Chem. 1996, 271:24684-24690.
doi: 10.1074/jbc.271.40.24684